Article ID: 1003－6326(2005)04－0863－05

Creep resistance of Mg-4%Al-2%RE-2%Ca alloy①

XUE Shan(薛　山)[1], SUN Yang-shan(孙扬善)[1], ZHU Tian-bai(诸天柏)[2], QIANG Li-feng(强立峰)[2], BAI Jing(白　晶)[1], ZHOU Jian(周　健)[1]
(1. Department of Materials Science and Engineering, Southeast University, Nanjing 210096, China; 2. Nanjing Welbow Metals Co Ltd, Nanjing 211221, China)

Abstract: The creep resistance of the alloy Mg-4Al-2RE-2Ca(AEC422) and the base alloy AE42 was studied. The results reveal that the precipitated phases of AEC422 consist of Al_2La and Al_2Ca by contrast with the precipitated phase $Al_{11}La_3$ in AE42, which is instable and decomposes to Al_2La and Al at high temperature. Creep resistance of AEC422 is significantly improved compared with that of AE42. The microstructure of AEC422 has no obvious changes after creep test at 175 ℃ and 70 MPa, as compared to that before creep test, indicating that Al_2La and Al_2Ca have high thermal stability. Especially Al_2Ca phase largely increases the strength of the grain boundaries in AEC422, which accounts for the creep resistance improvement.

Key words: creep resistance; grain boundaries sliding; intermetallic phase
CLC number: TG 146　　**Document code:** A

1 INTRODUCTION

The ternary AE42(Mg-4% Al-2% RE) alloy, in which RE mostly is lanthanum-rich or cerium-rich misch metal, shows good elevated temperature properties, excellent die castability and acceptable cost[1]. However, when the temperature is above 150 ℃, its creep resistance drops abruptly, which limits its further application in automotive industry[2].

Calcium additions have good effects on creep resistance of binary Mg-Al alloys[3, 4]. But nearly no results have been published in open literature on calcium addition into AE42 alloy yet. So the study on the combined strengthening effects of Ca and RE on Mg-Al based alloy will be of significance and interest.

In the present work, the quaternary Mg-4% Al-2% RE-2% Ca alloy(AEC422) shows much higher creep resistance than base alloy AE42 and the effect of RE and Ca on creep resistance is studied thoroughly.

2 EXPERIMENTAL

AEC422 alloy was melted in a mild steel crucible under the protection of a mixed gas atmosphere of 1% SF6 and 99% CO_2 (volume fraction). The rare earth elements used in the present investigation were lanthanum-rich misch metal(RELa-80, GB/T4153—93, Chinese Specification). Calcium addition was conducted by adding a master alloy with composition of Mg-30Ca(mass fraction, %). After the alloying elements were dissolved, the melt was held at 720 ℃ for about 15 min, then poured into permanent molds made of cast steel. Meanwhile, the base alloy AE42 was also prepared under the same condition for comparison. Dimension of the creep specimens was machined according to National Standard GB2039-80 and tested on the RD2-3 specified creep machine. Microstructures were characterized on selected specimens using optical microscope(OM) and scanning electron microscope(SEM). Microanalysis and determination of crystal structure of precipitates were carried out by X-ray energy dispersive spectroscopy(XEDS) and X-ray diffractometry(XRD), respectively.

3 RESULTS

3.1 X-ray diffraction

The XRD analyses of AE42 and AEC422 alloys were carried out and the diffraction patterns are shown in Fig. 1. All the peaks of AE42 are indexed to come from two distinct phases α-Mg and $Al_{11}La_3$ (Fig. 1(a)), which is consistent with the result in the previous investigation[5]. Two new peaks appearing in AEC422 alloy are identified as Al_2La and Al_2Ca (Fig. 1(b)). The results show that Ca additions not only lead to the formation of new aluminum-calcium intermetallic compound Al_2Ca phase, but also transform aluminum-RE in-

① **Foundation item:** Project(2001AA331030-01) supported by Hi-tech Research and Development Program of China; Project(BK2004208) supported by the Natural Science Foundation of Jiangsu Province, China
Received date: 2004－11－12; **Accepted date:** 2005－01－18
Correspondence: SUN Yang-shan, Professor; Tel: +86-25-83792454; E-mail: yssun@seu.edu.cn

termetallic phase from body centered $Al_{11}La_3$ phase to face centered Al_2La phase[6, 7].

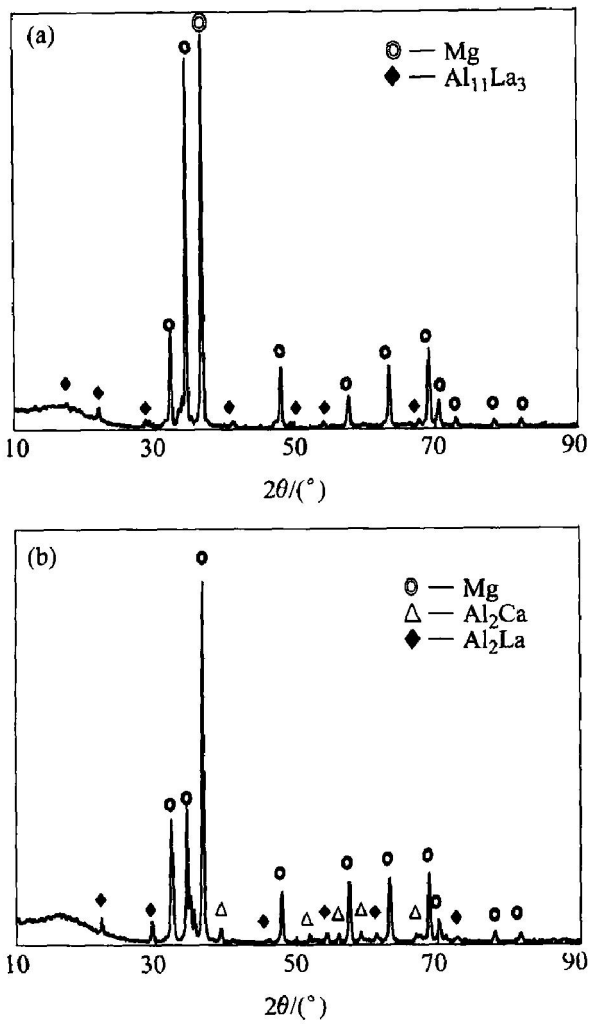

Fig. 1 XRD patterns of AE42(a) and AEC422(b) alloys

3.2 Microstructure

Fig. 2(a) shows an optical micrograph taken from the base alloy AE42, in which a large quantity of acicular intermetallic particles irregularly distribute in grains or at grain boundaries. The morphology of these particles is shown more clearly in the higher magnification image(Fig. 2(b)). Based on XRD pattern and results of XEDS microanalysis, these acicular particles are identified as $Al_{11}La_3$ with some cerium substituting lanthanum.

The microstructure of AEC422 alloy is quite different from that of AE42 under optical microscope(Fig. 3(a)). The acicular $Al_{11}La_3$ phase disappears and two new phases form in AEC422 alloy. XEDS analysis shows that the spotted phase contains La, Ce and Al elements, but the contents of La and Ce are much higher than those in $Al_{11}La_3$. The other is lamellar phase appearing at grain boundaries(Fig. 3(b)). The chemical composition of the lamellar phase determined by XEDS is approximately Al-31.7Ca-15.2Mg. Referring to the XRD pattern shown in Fig. 1(b), the spotted

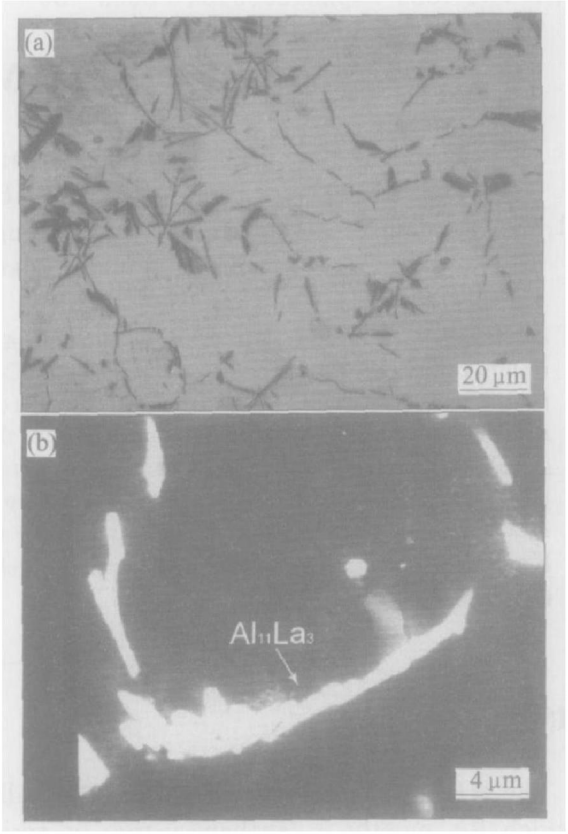

Fig. 2 Microstructures of as cast AE42 alloy
(a) —Optical image; (b) —SEM image

phase is determined as Al_2La and the lamellar phase is Al_2Ca. It can also be seen the distribution of Al_2La phase is irregular in grains or along grain boundaries, just the same as that of $Al_{11}La_3$ phase. However, the Al_2Ca phase is strictly precipitated along grain boundaries.

3.3 Creep properties

The creep tests of the two alloys were carried out under the temperature of 175 ℃ and applied stress of 70 MPa. The creep curves are shown in Fig. 4, from which the total time-dependent strain measured and the steady creep rate calculated are marked. Under the condition used in the present investigation, the creep resistance of AE42 alloy seems quite poor. The total strain and the steady creep rate are 7.75% and 2.77×10^{-7}/s respectively after creep rupture at about 61 h finally. 2.0% (mass fraction) calcium additions lead to significant improvement of creep resistance of AEC422 alloy. The total strain of AEC422 alloy is only 0.76% after 100 h creep, one order of magnitude lower compared with that of AE42. The steady creep rate gets to 5.54×10^{-9}/s, two orders of magnitude less than that of AE42.

3.4 Microstructure of specimens after creep test

The fractograph of AE42 specimen after creep fracture is shown in Fig. 5(a), from which it can be seen that AE42 alloy ruptures along grain boundaries after creep test. Meanwhile, a large

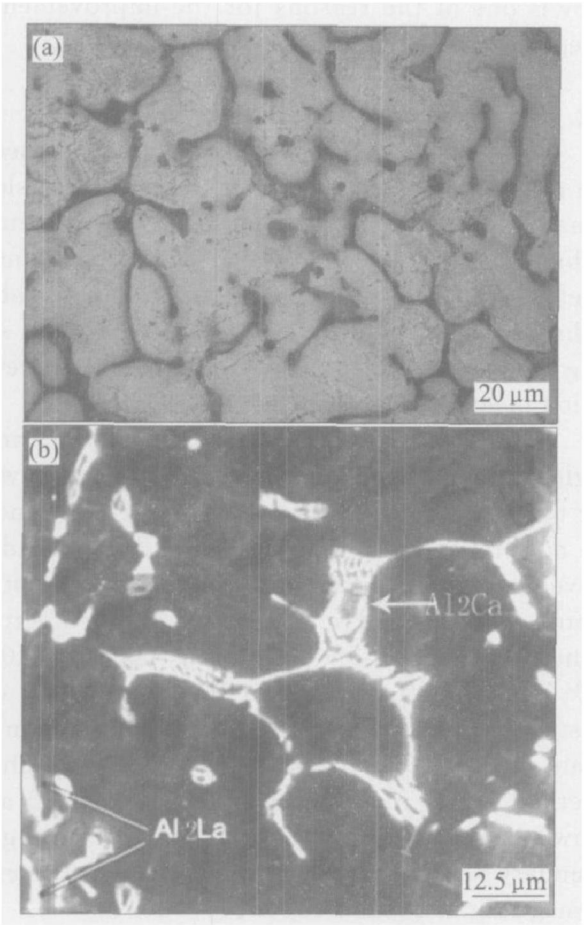

Fig. 3 Microstructures of as cast AEC422 alloy
(a) —Optical image; (b) —SEM image

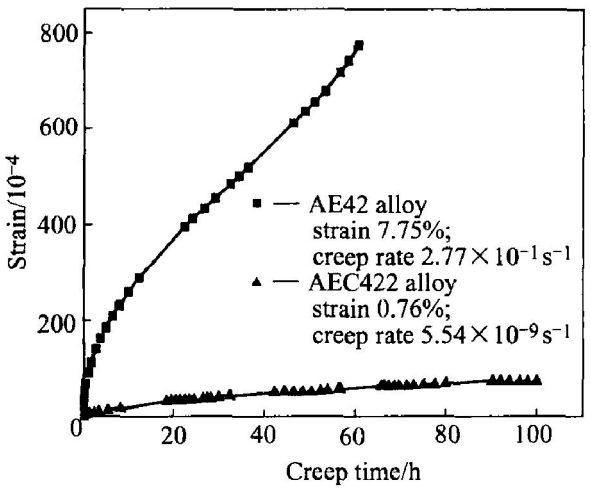

Fig. 4 Creep curves of alloys at 175 ℃ and 70 MPa

number of new collective particles form in the microstructure after creep instead of the acicular $Al_{11}La_3$ phase. The shape of these granular particles appears actually short rod-like under high magnification (Fig. 5(b)). XEDS analysis performed on these particles shows that the mass fractions of Al and (La+ Ce) are 24.15% and 65.95%, respectively. So this new phase can be identified as Al_2La combining with the previous investigations[5, 8]. Microanalysis also reveals some gray particles(Fig. 5(b)), in which only Mg and Al exist and the Mg/Al molar ratio is about (1.3-1.5)/1, thus, the phase is identified as $Mg_{17}Al_{12}$ (β), which commonly appears in Mg-Al based alloys.

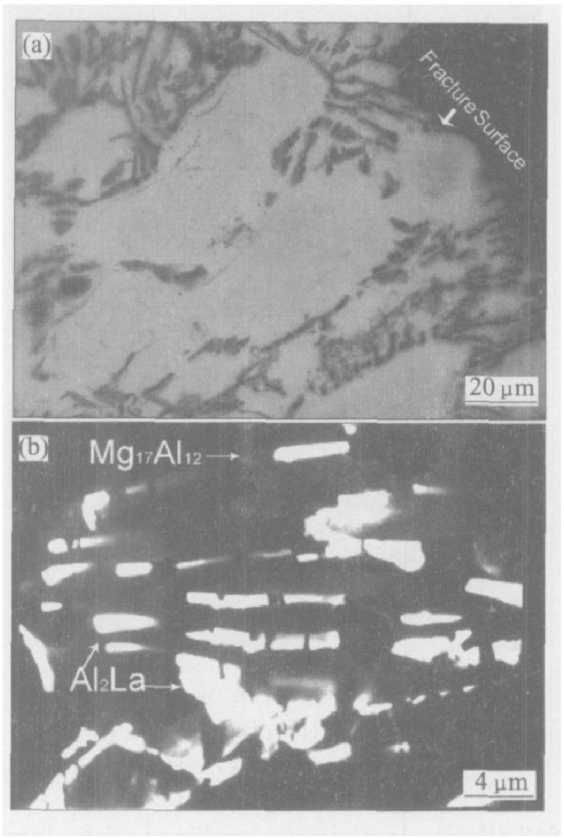

Fig. 5 Microstructures of AE42 alloy after creep
(a) —Optical image; (b) —SEM image

For alloy AEC422, 100 h creep test does not result in obvious changes in microstructure, as shown in Fig. 6(a) and Fig. 6(b). The shape and size of grains after creep keep the same as those of as cast and the precipitation process. Neither the spotted Al_2La phase nor the lamellar Al_2Ca phase undergoes any change, indicating high structure stability of this alloy.

4 DISCUSSION

The fact that the creep resistance of AEC42 alloy is much higher than that of the base alloy AE42 attributes to two factors as follows.

4.1 Transformation of rare earth precipitated phase

The atom radius of Mg and La are 1.6 Å and 1.877 Å respectively and $\Delta r/r = 17.3\%$, which can not meet the requirement for the formation of the solid solution according to Hume-Rothery Rule ($\Delta r/r < 15\%$). Lanthanum element has nearly no solid solubility in αMg according to Mg-La binary phase diagram[9]. In Mg-4Al-2La ternary system (AE42 alloy), lanthanum combines with aluminum

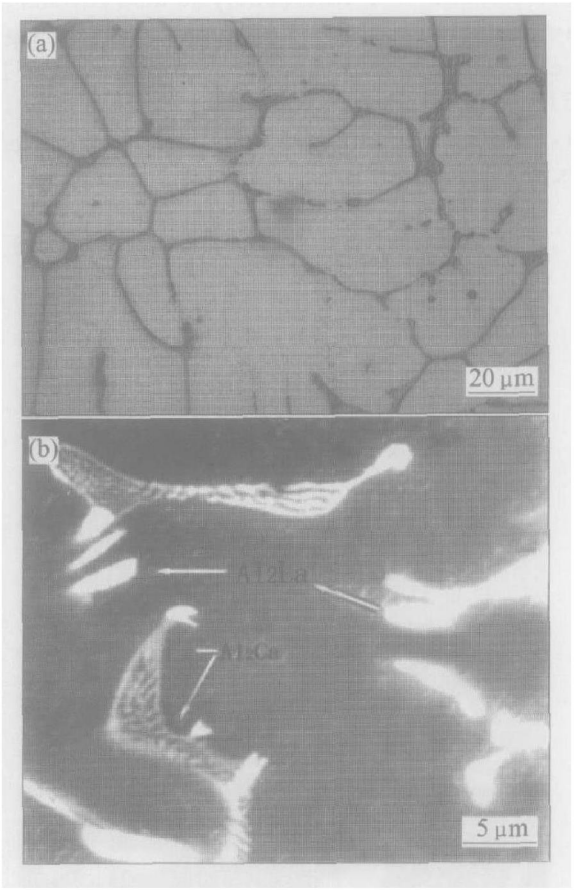

Fig. 6 Microstructures of AEC422 alloy after creep
(a) —Optical image; (b) —SEM image

to form $Al_{11}La_3$ phase in the present investigation. However, $Al_{11}La_3$ is not a stable phase and decomposes when the temperature is above 150 ℃[5]:

$$Al_{11}La_3 \rightarrow 3Al_2La + 5Al \quad (1)$$

then the released aluminum reacts with Mg to form $Mg_{17}Al_{12}$ phase:

$$12Al + 17Mg \rightarrow Mg_{17}Al_{12} \quad (2)$$

two formulas above are combined as

$$Al_{11}La_3 + Mg \rightarrow Al_2La + Mg_{17}Al_{12} \quad (3)$$

The $Mg_{17}Al_{12}$ phase (β phase) has a low melting point (437 ℃) and can readily soften and coarsen due to accelerated diffusion with increase of temperature[10], which greatly weakens the grain boundaries. The formation of β phase is a key factor accounting for the low creep resistance in Mg-Al base system.

However in AEC422 alloy, calcium firstly combines with aluminum to form the thermally stable Al_2Ca phase (melting point of 1 079 ℃), which implies the free energy of Al_2Ca phase is lower than that of Al-La intermetallic phase. Then, the consumption of aluminum content through the formation of Al_2Ca promotes the Al-La intermetallic phase to transform from previous $Al_{11}La_3$ in AE42 alloy to Al_2La in AEC422 alloy. Therefore, the formation of the thermally stable Al_2La phase instead of unstable $Al_{11}La_3$ in AEC422 alloy is one of the reasons for the improvement of creep resistance of AEC422 alloy.

4.2 Strengthening grain boundaries

Mg-Al base alloys with hexagonal structure can not afford enough sliding systems for dislocations to slip during deformation. Grain boundary sliding supplies two additional sliding systems to meet deformation requirement[11]. Grain boundary sliding with a model of dislocation climb and slipping has ever been investigated elsewhere[12], which meets the experiment very well.

Generally, the grain boundary sliding can be neglected at ambient temperature. However, when the temperature rises, the atoms at grain boundary are not stable and prone to diffuse, which leads to movement of the grain boundary under the stress during the creep. Humble found in their experiment that grain boundary sliding takes up 40%–80% in total deformation in Mg-0.8Al% by contrast with less than 10% in pure aluminum[13]. Grain boundary sliding leads to the intergrannular fracture finally just as the fracture of AE42 alloy shown in Fig. 5(a). The result indicates the grain boundary sliding plays a primary role in the creep of magnesium based alloy[14].

In the present investigation, either $Al_{11}La_3$ phase or Al_2La phase is randomly distributed in grains or at grain boundaries. The strengthening effect to grain boundaries through RE element added into Mg-Al based alloy can inhibit the precipitation of β phase at grain boundaries during solidification. Furthermore, $Al_{11}La_3$ phase is unstable when temperature is above 150 ℃, which directly deteriorates the strength of the grain boundaries and results in the dropdown of creep resistance. But the lamellar Al_2Ca phase in AEC422 alloy precipitated along grain boundaries can strengthen the grain boundaries to the most degree[15]. The presence of the thermostable Al_2Ca phase at grain boundary provides effective pinning to resist grain boundary sliding and climb and improves the creep resistance of AEC422 significantly.

5 CONCLUSIONS

1) The precipitated phases in AEC422 alloy are spotted Al_2La and lamellar Al_2Ca phases by contrast with the acicular $Al_{11}La_3$ phase dominated in the base alloy AE42 alloy.

2) AEC422 alloy shows excellent creep resistance, whose secondary creep rate gets to 5.54×10^{-9}/s at 175 ℃ and 70 MPa, two orders of magnitude less than that of AE42 alloy.

3) The microstructure of AEC422 is very stable during creep test. However, the microstructure of AE42 changes largely after creep on the other hand. The poor creep resistance of AE42 al-

loy attributes to the decomposition of $Al_{11}La_3$ phase at high temperature.

4) The high creep resistance of AEC422 is largely due to the thermally stable Al_2Ca phases distributed at grain boundaries, which impedes the grain boundary sliding in creep.

REFERENCES

[1] LU Yi-zhen, WANG Qu-dong, ZENG Xiao-qin, et al. Effect of rare earth on the microstructure properties and fracture behavior of Mg-Al alloys [J]. Materials Science and Engineering A, 1999, 278(1, 2): 66-76.

[2] Powell B. Development of GM calcium-containing, creep-resistant magnesium alloys for powertrain applications [A]. DING Wei-nan. Sinomag Die Casting Magnesium Seminar [C]. Beijing, 2002. 14-25.

[3] Pekguleryuz M, Baril E. Creep resistance magnesium diecasting alloys based on alkaline earth elements [J]. Materials Transactions, 2001, 7(42): 1258-1267.

[4] Koray O, YU Zhong, LIU Zi-Kui, Computational thermodynamics and experimental investigation of Mg-Al-Ca [A]. Hryn J. Magneium Technology 2001[C]. New Orlands: Minerals, Metals & Materials Society, 2001. 113-119.

[5] Powell B, Vadim R, Michael P, et al. The relationship between microstructure and creep behavior in AE42 magnesium die casting alloy [A]. Hryn J. Magnesium Technology 2001[C]. New Orlands: Minerals, Metals & Materials Society, 2001. 175-181.

[6] American Society for Metals Metals Handbook [M]. Ohio: Metals Park, 1973.

[7] DU Wen-wen, SUN Yang-shan, MIN Xue-gang. Microstructure and mechanical properties of Mg-Al based alloy with calcium and rare earth additions [J]. Materials Science and Engineering A, 2003, 356: 1-7.

[8] Moreno P, Nandy T, Jones J, et al. Microstructure and creep behavior of a die cast magnesium rare earth alloy [A]. Kaplan H I. Magnesium Technology 2002 [C]. Seattle: Minerals, Metals & Materials Society, 2002. 111-116.

[9] Gschneidner K, Binary alloy phase diagrams [A]. Backer H. Alloy Phase Diagrams[C]. Ohio: ASM International, 1992. 2-43.

[10] Bradi D, Kadi-hannifi M. The kinetics of the discontinuous precipitation and dissolution on Mg-Al alloys [J]. Journal of Materials Science, 1999, 34: 5331-5336.

[11] Pekguleryuz O. Creep resistance magnesium alloys for powertrain applications [J]. Advanced Engineering Materials, 2003, 12(5): 866-878.

[12] Spigarell S. Creep of a thixoformed and heat treated AZ91 Mg-Al-Zn alloy [J]. Scripta Mater, 2000, 42: 397-402.

[13] Humble P. Towards a cheap creep resistant magnesium alloy [J]. Materials Forum, 1997, 21: 45-56.

[14] Luo A. Recent magnesium alloy development for elevated temperature applications [J]. International Materials Reviews, 2004, 21: 13-30.

[15] Bamberger B, Jardim P, Solorzano G. Precipitation hardening in Mg-Zn-Ca alloys [A]. Kaplan H I. Magnesium Technology 2002[C]. Seattle: Minerals, Metals & Materials Society, 2002. 75-79.

(Edited by YANG Bing)